65235

OCTOBER

1965

ROYAL AIRCRAFT ESTABLISHMENT

TECHNICAL REPORT No. 65235

AN EXPLORATORY INVESTIGATION INTO THE DEFLECTION OF THICK JETS BY THE COANDA EFFECT

by

L. J. S. Bradbury

M. N. Wood

MINISTRY OF AVIATION

FARNBOROUGH HANTS

U.D.C. No.532.525.2 : 532.5.011.17 : 533.694.7

ROYAL AIRCRAFT ESTABLISHMENT

Technical Report No.65235

October 1965

AN EXPLORATORY INVESTIGATION INTO THE DEFLECTION OF THICK JETS BY THE COANDA EFFECT

by

L. J. S. Bradbury
M. N. Wood

SUMMARY

Measurements have been made of the maximum deflection from the Coanda effect of a plane jet by a deflecting surface comprising a circular drum whose diameter was four times the jet nozzle width and which had a small flap attached to it. It was shown that the deflection of this comparatively thick jet is dependent on the jet pressure ratio and only quite small deflections can apparently be obtained for pressure ratios greater than 2. A few tests with a jet of slightly reduced thickness showed that although larger deflections were obtained at low pressures, only small deflections were again possible at pressure ratios greater than 2. Finally, some attempts at boundary layer control with spanwise auxiliary blowing slots on the deflecting surface indicated that some increase in deflection angles may thereby be achieved.

Departmental Reference: Aero 2756

CONTENTS

		Page
1	INTRODUCTION	3
2	INITIAL CONSIDERATIONS	3
3	MODEL DETAILS	5
4	TESTS WITH NO AUXILIARY BLOWING	5
5	TEST WITH AUXILIARY BLOWING	8
6	CONCLUDING REMARKS	9
ACKNOWLEDGEMENT		9
Appendix A	Simple inviscid theory for flow over a deflecting surface	10
Symbols		12
References		13
Illustrations		Figures 1-12

1 INTRODUCTION

The Coanda effect in which jets adhere or tend to adhere to adjacent surfaces is becoming of increasing interest due to its relevance to such devices as jet flaps, thrust augmenters and fluid computing units. Most of the work on this subject has been carried out on plane jets with a thickness small compared with the radius of curvature of the deflecting surface and where deflections of over 180° are obtainable (see, for example, Newman[1]). There is however some interest in thick jet deflection and the present investigation was carried out as a preliminary exploration of this problem. It should be stressed at the outset that the present investigation was intended primarily to provide information on which a future programme could be more realistically planned and, in consequence, the experiments were comparatively limited in scope. The results should therefore be applied with some caution.

Section 2 outlines the dimensional framework against which the problem is set and the broad features of the flow are discussed. Section 3 then gives details of the model used in the experiments and, finally, the results obtained are discussed in Sections 4 and 5.

2 INITIAL CONSIDERATIONS

In Fig.1, the 'ideal' model in which we are interested is shown schematically. It consists of a parallel-sided nozzle (width h) exhausting over a deflecting surface comprising a circular drum (radius R) with a straight flap (length L) attached tangentially to it. Some basic general relationships can first be usefully formulated for a two-dimensional model with fixed values of the parameters h/R and L/R. For the static pressure distribution P_1 on the deflecting surface and the flap angle θ°_{sep} at which the jet separates from the deflecting surface, dimensional arguments for air jets with an ambient stagnation temperature give

$$\frac{P_1}{P_\infty} = \text{function of} \left(\frac{P_P}{P_\infty}, \ (R_e)_P, \ \theta, \ x/h \right)$$

$$\theta^\circ_{sep} = \text{function of} \left(\frac{P_P}{P_\infty}, \ (R_e)_P \right)$$

where P_P and P_∞ are the primary jet supply pressure and atmospheric pressure respectively, $(R_e)_P$ is a relevant jet Reynolds number which, for present purposes, need not be defined precisely, x is the distance along the

deflecting surface from some suitable reference point (say the jet nozzle) and θ is the flap angle as defined in Fig.1.

At high Reynolds numbers, it is well known that flows tend to become independent of Reynolds number and the effect of variation of this parameter can then be ignored. In addition, at very low values of the primary jet supply pressure, the flow may be treated as incompressible and only pressure differences are then important. With these simplifications,

$$\frac{P_1 - P_\infty}{P_P - P_\infty} = \text{function of } (x/h, \theta)$$

and

$$\theta^\circ_{sep} = \text{a constant.}$$

These functions can only be properly determined at this stage from experiments but, in Appendix A, some consideration is given to the case of an inviscid flow over a deflecting surface. A very simple theory is there developed which leads to the conclusion that the pressure distribution over the deflecting surface and the velocity distribution through the jet in such an inviscid flow will be similar to those shown schematically in Figs.2(a) and 2(b). The effect of viscosity will be to introduce a turbulent boundary layer onto the deflecting surface and a free mixing layer at the outer edge of the flow. The resulting modification to the inviscid velocity profile is shown in Fig.2(b). If the jet is thin in relation to the drum radius, these two turbulent shear layers will coalesce, resulting in a flow similar to that already studied by Newman[1]. The outward spread of the jet due to turbulent mixing will cause an adverse pressure gradient along the deflecting surface and this can lead eventually to flow separations. Alternatively, flow separations may occur as a result of the adverse pressure gradient encountered by the flow at the junction of the circular drum with the straight flap.

When the flow is incompressible, the flap angle at which the jet separates from the deflecting surface should be sensibly constant as already discussed. As the jet pressure ratio, P_P/P_∞, is increased, compressibility effects will begin to make themselves felt and, finally, regions of supersonic flow will appear on the deflecting surface and the consequent shock waves can lead to the possibility of shock induced separations.

In an effort to suppress or delay flow separations and hence increase the maximum deflection of the jet, boundary-layer control by means of a thin auxiliary jet exhausting tangentially from the deflecting surface seemed worth

investigating. The effectiveness of this auxiliary jet depends not only on its pressure ratio and mass flow relative to the main jet but also on its position in relation to the adverse pressure gradients.

3 MODEL DETAILS

The model used in these tests (Fig.3) consisted of a fixed geometry contraction and nozzle at the exit of which was mounted the deflecting surface. This surface comprised a circular drum with a slightly concave flap fixed to it. The drum and flap assembly could be rotated continuously about the drum centre. There were, in fact, three alternative drum and flap assemblies which differed from one another only in the auxiliary blowing arrangements. Model 1 was a plain drum and flap with no auxiliary blowing slot. Models 2 and 3 each had one full span auxiliary blowing slot 0·025 inch wide fixed in the positions on the drum surface shown in Fig.3. All three models were fitted with small endplates, also shown in Fig.3. The ratio of drum radius to primary jet width was 2 and the primary jet aspect-ratio was 10.

There were two chordwise rows of static holes on the deflecting surface of Model 1, one on the centre-line and the other 1·25 inches to one side of it. There were four static holes per row at 0·2 inch, 1·2 inches, 2·2 inches and 3·2 inches respectively from the flap trailing-edge. Models 2 and 3 also had two "rows" of static holes but with only two holes per row at 0·2 inch and 1·2 inches respectively from the flap trailing-edge.

The air supplies to the primary and auxiliary jets were independent of one another, both air supplies being approximately at ambient temperature i.e. 'cold' jets.

Certain features of the model design were determined by other considerations in addition to the requirements of the present investigation and the model departed considerably from the 'ideal' model of Fig.2. The nozzle walls were non-parallel and curved with the result that the jet exit angle was not known with any precision. This, in combination with the concave flap, made it difficult to define precisely the effective flap angle. The model was not, therefore, particularly suitable for the purposes of the present investigations but its ready availability enabled some results to be obtained quickly in advance of the construction of a new special model.

4 TESTS WITH NO AUXILIARY BLOWING

Because of the unusual geometrical configuration of the model, it is necessary at the outset to define the meaning of the actual flap angle, $\hat{\theta}$,

as distinct from the flap angle, θ, of the idealised model of Fig.2. The datum or zero flap angle on this model was taken for convenience as the position of the flap and drum shown in Fig.3(b) and flap angles are measured relative to this position. It is important to note that zero flap angle does not correspond with zero jet angle as will be shown subsequently and, therefore, care must be exercised in interpreting the present results in relation to the performance of a model similar to the 'ideal' model of Section 2. This point will be discussed later.

The initial tests which were very simple, consisted mainly of measuring the flap angle, $\hat{\theta}$, at which the jet separated from and re-attached to the flap. This separation was well defined because of the sudden change in noise, thrust vector and static pressure on the flap surface that would accompany separation. In Fig.4 is shown a typical variation of static pressure at a fixed point on the flap surface as the flap angle was increased through the point where separation occurred. It is to be noted that this static pressure variation is the same both on the centre-line and 1·25 inches from the centre-line. This suggests that spanwise variations in the flow were small; this was further confirmed by some spanwise pitot-static traverses which showed that spanwise variations were confined to the outer 1/2 inch of the flap even immediately prior to separation*.

In Fig.5 is shown the variation of separation angle with primary supply pressure for the three models. For $1 < P_p/P_\infty \leq 1{\cdot}25$, models 1 and 3 exhibited an apparently constant separation angle of about 65° in accordance with equation (2). The rather odd behaviour of model 2 must be a Reynolds number effect associated with the surface flow over the auxiliary blowing slot and indicates that some caution should be exercised in applying the principle of Reynolds number similarity to flows containing a low Reynolds number 'component'- in this case, the flow over the small auxiliary blowing slot. It should be mentioned that the auxiliary blowing slot was not open to atmospheric pressure so that air was not being drawn in through the slot during these tests. At higher pressures ($P_p/P_\infty \geq 1{\cdot}5$), all three models behaved in a similar fashion and showed that the separation angle decreased with increasing supply pressure.

The flap angles at which the jet-re-attached having first separated from the flap were, with one notable exception, several degrees less than the separation flap angles. The exception was found with model 2 which showed

---

* The effect of additional end plates was checked very roughly by clamping large metal plates against the edge of the model. No appreciable effect on the results of the various tests could be observed.

pronounced hysteresis effects in the pressure range $1 < P_p/P_\infty \leq 1{\cdot}5$. For example, at $P_p/P_\infty \approx 1{\cdot}0$, the re-attachment angle was between 65° and 70° and it is noteworthy that this is practically identical with the separation angle of the other models at this pressure.

In order to check that the small concavity of the flap did not affect the results, it was smoothed over with Plasticine. No measurable effect could be observed.

The problem of relating the present results to the 'ideal' model discussed in Section 2 is that the jet angle with no Coanda deflection is unknown. However, from the geometry of the model - Fig.3(b) - it would seem that with the flap and drum removed so that there was no Coanda deflection, the jet would exhaust at an angle of about 30° (or somewhat less) to the model axis. Now, it was found that with the flap at the datum or 'zero' position, the jet angle was already 10° to the model axis* so that for a jet angle of 30°, the flap angle would be 20°. Therefore, very crudely, we can estimate the separation angles on the 'ideal' model by reducing the flap angles at separation measured on the present model by 20°. Notwithstanding the fact that this procedure is likely to be somewhat pessimistic, it is now clear from reference to Fig.5 that the Coanda deflection of the jet for $P_p/P_\infty \geq 2{\cdot}5$ is small.

In addition to the above tests, the limited number of static holes enabled some idea of the flow over the flap to be obtained. In Fig.6 are shown results of these measurements on Model 1 for two values of primary supply pressure ($P_p/P_\infty = 1{\cdot}7$ and $2{\cdot}4$), and a range of flap angles. It should be stressed that the curves drawn through the points in Fig.6 are intended only to clarify the diagram. The actual pressure distributions were probably more angular and similar to the schematic pressure distribution shown in Fig.2. The non-parallel curved nozzle and the concave flap are undoubtedly responsible for the existence of the strong pressure gradients within the nozzle and also the positive (above atmospheric) pressures on the flap. To this extent, the results are not very useful since they are strongly dependent on the particular geometry of the model. However, the existence of the adverse pressure gradient on the flap is clearly shown and the collapse of the high suctions when the jet separates is also demonstrated. It is also to be noted that the Mach number on the drum surface apparently exceeds unity even when $P_p/P_\infty = 1{\cdot}7$.

---

* This angle was obtained initially from some pitot-static traverses in the jet away from the model. However, it was later confirmed by balance measurements of the thrust vector of the model.

At a later stage in the experiments, it proved possible to mount the model on a balance so that thrust measurements could be made*. Fig.7 shows the relationship between the angle of the thrust vector and the flap angle for Model 1 for pressure ratios of 1·3 and 1·5. For this model, the results may clearly be represented up to separation by

$$(\text{thrust vector angle})^\circ = (\text{flap angle})^\circ + 10^\circ$$

The ratio of the resultant thrust to the resultant thrust at zero flap angle, Fig.8, shows that the maximum loss of resultant thrust is about 10 per cent and occurs just before separation. It should be noted that no measurable change in the mass flow occurred with variations of the flap angle at constant supply pressure.

To conclude the series of measurements, the thickness of the jet was reduced from 1/2 inch to 5/16 inch (giving $R/h = 3{\cdot}2$) by partially filling the jet slot with resin glue. The results of tests for the flap angle at separation on this model are shown in Fig.9. The outstanding feature here is that although large gains in separation angle were obtained at low pressures, the separation angles at the highest pressures were almost unaffected by the reduction in the primary jet width.

Subsequent balance measurements with $R/h = 3{\cdot}2$ are shown in Fig.10. In this case, the results up to separation may be summarized by the expression

$$(\text{thrust vector angle})^\circ = 1{\cdot}04\ (\text{flap angle})^\circ + 10^\circ$$

It is surprising to find that the slope here is apparently greater than 1·0! A maximum loss of resultant thrust of about 10 per cent was again observed (Fig.11).

5 TESTS WITH AUXILIARY BLOWING

Attempts to carry out measurements with auxiliary blowing soon revealed that the model was not really adequate to undertake such measurements. In the first place, the separation phenomenon was not so well defined as previously and, moreover, spanwise variations in the width of the auxiliary blowing slot led to gross asymmetries in the flow. Both of these factors confused the results and, consequently, only the simple measurements of flap angle at separation were attempted.

---

* With the model mounted on the balance, there were restrictions in the air supply so that a pressure ratio higher than 1·5 was not obtainable. In addition, the mounting restricted the maximum flap angle to 100°.

In Fig.12 are shown the flap angles at apparent separation for three values of primary jet supply pressure (P_p/P_∞ = 1·7, 2 and 2·4) on models 2 and 3 respectively over a range of auxiliary jet supply pressures. It would appear that for $P_p/P_\infty \geq 2$, the auxiliary jet had very little effect. However, below this primary jet supply pressure, large increases in the flap angle at separation were obtained though these gains appeared to depend critically on the position of the auxiliary blowing slot. Clearly, the effect of auxiliary blowing deserves further attention but, for the reasons given above, this must await a further and more suitable model which is now under construction.

For completeness, nominal values of both the primary and auxiliary jet thrusts are quoted in Fig.12. These values were obtained theoretically by assuming an isentropic expansion from the supply pressure to atmospheric pressure and they give a rough guide to the relative magnitudes of the primary and auxiliary jet thrusts.

6 CONCLUDING REMARKS

The present simple experiments have shown that the deflection of a comparatively thick jet by the Coanda effect is possible, but the degree of turning depends quite strongly on the pressure ratio of the jet, while for values greater than 2, only small deflections can be obtained. The possibility of improving the turning effectiveness by the use of a thin auxiliary jet exhausting from the deflecting surface was investigated and it was apparent that, at primary jet pressure ratios somewhat below 2, substantial increases in jet deflection angle were obtainable although they depended critically on the position of the auxiliary blowing slot. These tests were sufficiently encouraging to warrant a further investigation, so further work is being carried out on two more elaborate models. Both of these models closely correspond to the 'ideal' model discussed in Section 2 and they will enable the effects of a wide range of geometrical parameters to be studied. Only one model has provision for auxiliary blowing; on the other model, there are greater facilities provided for studying the structure of the flow. The two models will therefore provide information which is complementary.

ACKNOWLEDGEMENT

B.A.C. (Weybridge) made available the simple model used in the tests described in this Report.

Appendix A

SIMPLE INVISCID THEORY FOR FLOW OVER A DEFLECTING SURFACE

Exact inviscid theories for the flow of a jet over a deflecting surface have been developed comparatively recently[2]. However, in order to illustrate some of the broad features of such a flow, a very simple analysis can be carried out.

It is assumed that at each position on the deflecting surface, the flow is similar to a non-separating constant thickness jet flowing around a circular cylinder having the same radius of curvature at that position. Thus, there is a simple equilibrium between centrifugal forces and the radial pressure gradients. Hence

$$\frac{\partial P}{\partial y} = \frac{\rho U^2}{R + y} \qquad (A.1)$$

where R is the local radius of curvature of the deflecting surface and y is the distance from and normal to this deflecting surface. For simplicity, an inviscid incompressible flow will be considered. Thus

$$P + \frac{1}{2}\rho U^2 = P_P, \text{ a constant.} \qquad (A.2)$$

From equations (A.1) and (A.2), we obtain

(a) $$C_P = \frac{P - P_\infty}{P_P - P_\infty} = 1 - \left(\frac{R + \delta}{R - y}\right)^2 \qquad (A.3)$$

where δ is the y-ordinate at the edge of the jet where $P = P_\infty$.

(b) $$\frac{U}{U_\infty} = \frac{R + \delta}{R + y} \qquad (A.4)$$

where U_∞ is the velocity at the edge of the jet where $y = \delta$.

(c) from mass flow continuity

$$h_\infty = (R + \delta) \log\left(\frac{R + \delta}{R}\right) \approx \delta \left\{1 + \frac{\delta}{R} - \frac{1}{6}\left(\frac{\delta}{R}\right)^2 + O\left(\frac{\delta}{r}\right)^3\right\} \text{ if } R > \delta \qquad (A.5)$$

and where h_∞ is the width of the nozzle exhausting the same mass flow rate to atmospheric pressure. This expression shows that $h_\infty \geq \delta$ for all positive values of R.

From equation (A.3), the pressure coefficient on the deflecting surface becomes

$$C_{P_1} = 1 - \left(\frac{R + \delta}{R}\right)^2 . \qquad (A.6)$$

If there is a discontinuity in R, at the drum-flap junction for example, equations (A.5) and (A.6) give a discontinuity in both δ and C_{P_1} which is obviously unrealistic and is due to the initial simplifying assumption embodied in equation (A.1). In the case of an exact inviscid solution, no such discontinuity would arise and a pressure distribution similar to that shown in Fig.2(a) would be obtained. However, provided there is a reasonable length of flow over the circular drum, the simple expressions obtained from the present simple analysis should be in good agreement with an exact inviscid solution over this drum region of the flow. Thus, in this region, inviscid velocity distributions through the jet will be given by equation (A.4) which gives rise to velocity distributions of the sort shown schematically in Fig.2(b).

SYMBOLS

R	radius of circular drum
L	flap length
h	width of jet nozzle
δ	local jet thickness
P_P	primary jet supply pressure
P_A	auxiliary jet supply pressure
P_∞	atmospheric pressure
P_1	static pressure on the deflecting surface
P	static pressure in the jet
n	P_P/P_∞
θ	'ideal' flap angle
$\hat{\theta}$	model flap angle
θ_{sep}	flap angle when the flow separates from the deflecting surface
$(Re)_P$	primary jet Reynolds number
U	jet velocity
U_∞	jet velocity at atmospheric pressure
x	distance along the deflecting surface from the jet nozzle
y	distance normal to the deflecting surface
C_P	pressure coefficient
C_{P_1}	pressure coefficient on the deflecting surface
ρ	air density
M	Mach number
h_∞	defined in Appendix A - equation (A.5)
T	jet thrust
T_o	jet thrust at zero flap angle

REFERENCES

No.	Author	Title, etc.
1	B. G. Newman	Deflection of a plane jet by adjacent boundaries - Coanda effect. Boundary Layer and Flow Control, Vol.1, Pergamon Press 1961
2	Th. E. Labriyere P. J. Zandbergen	Potential theoretical description of the flow in a jet deflected by a circular cylinder - Coanda effect. NLR-TN G.31 1963

Fig.1&2

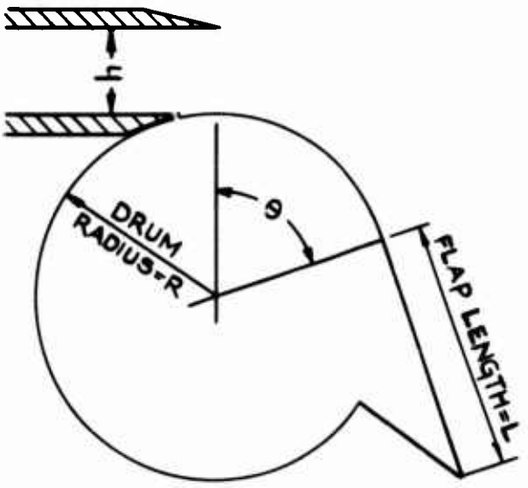

FIG.1 THE IDEAL MODEL

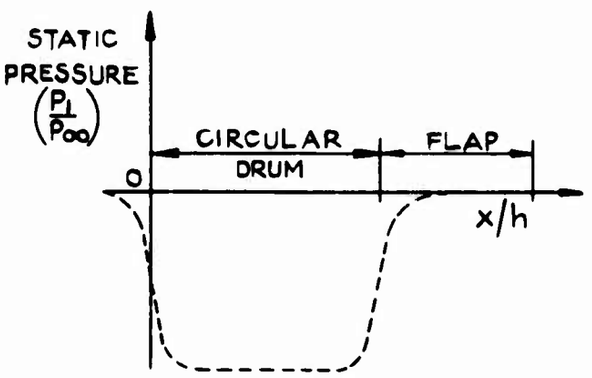

(a) INVISCID FLOW PRESSURE DISTRIBUTION ON THE DEFLECTING SURFACE

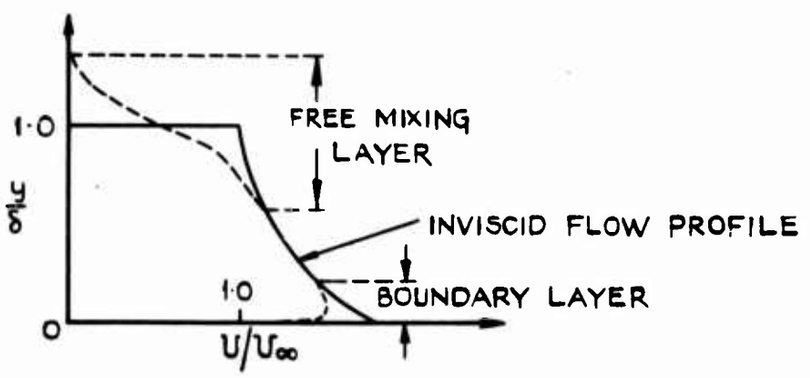

(b) VELOCITY DISTRIBUTION ACROSS THE JET SHOWING THE EFFECT OF TURBULENT MIXING

FIG. 2 SCHEMATIC REPRESENTATION OF THE FLOW OVER THE DEFLECTING SURFACE

Fig.3

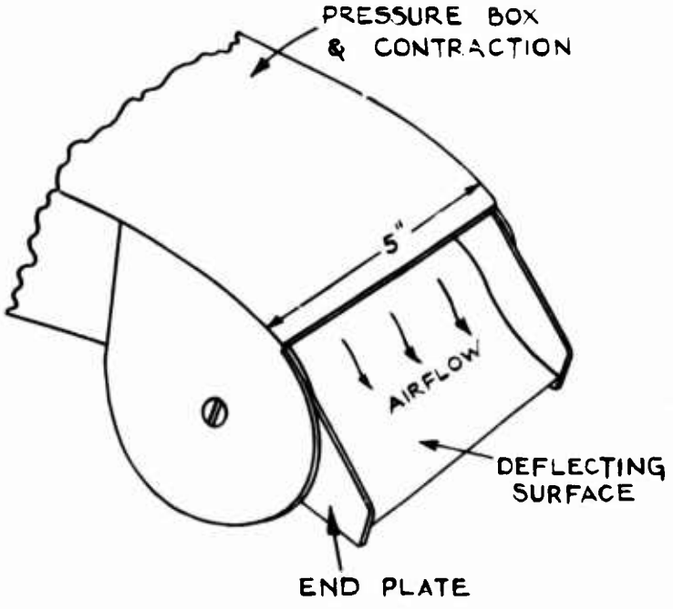

(a) SCHEMATIC DIAGRAM OF MODEL

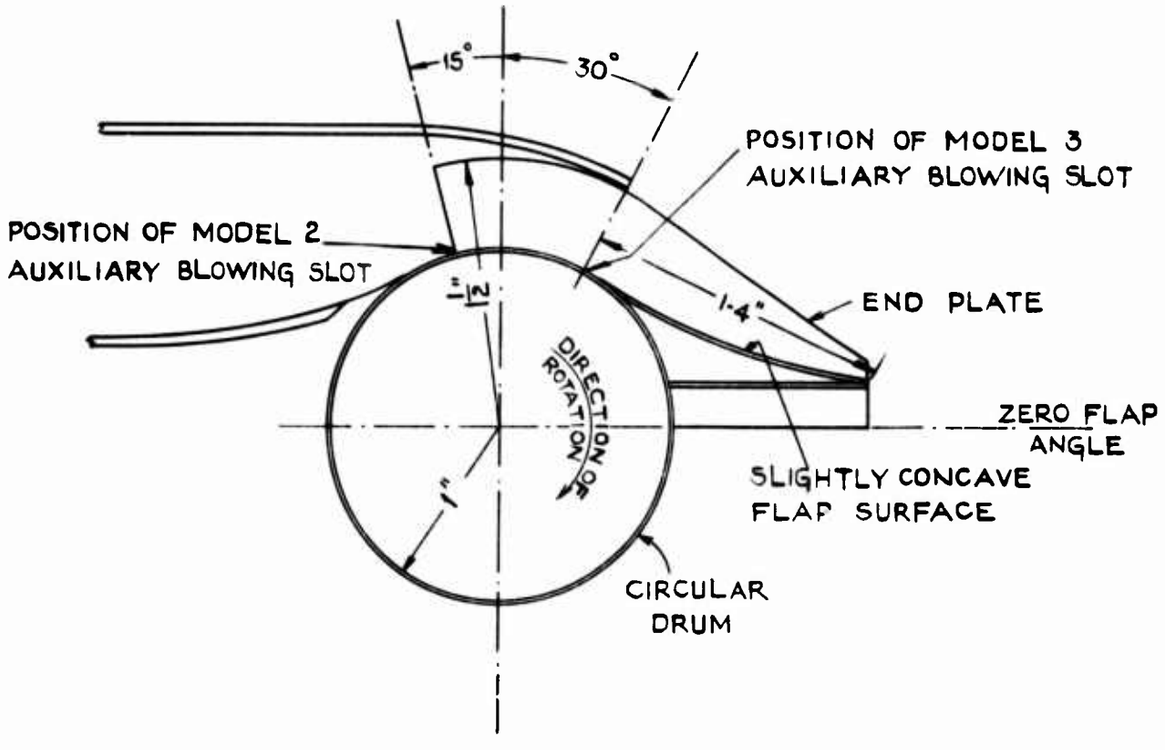

(b) CROSS SECTION THROUGH THE DEFLECTING SURFACE & CONTRACTION

FIG.3 DETAILS OF MODEL

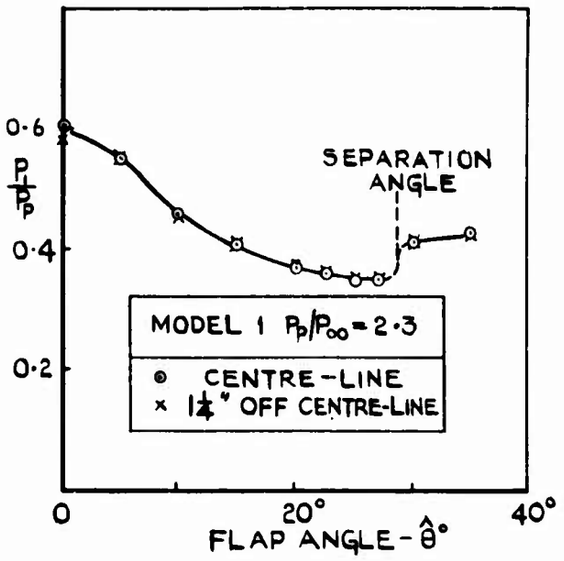

FIG.4 VARIATION OF STATIC PRESSURE WITH FLAP ANGLE AT 1·2" FROM THE TRAILING EDGE

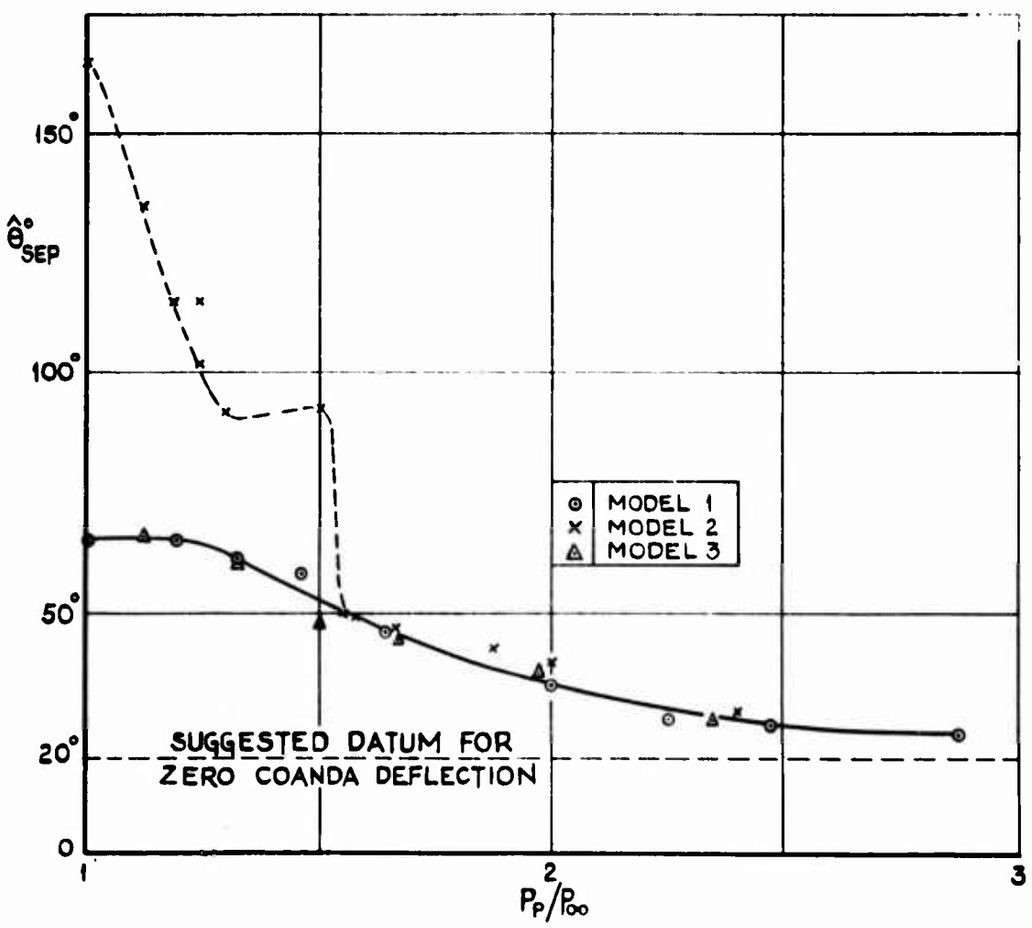

FIG. 5 FLAP ANGLE AT SEPARATION - R/h = 2

Fig.6

47354 S

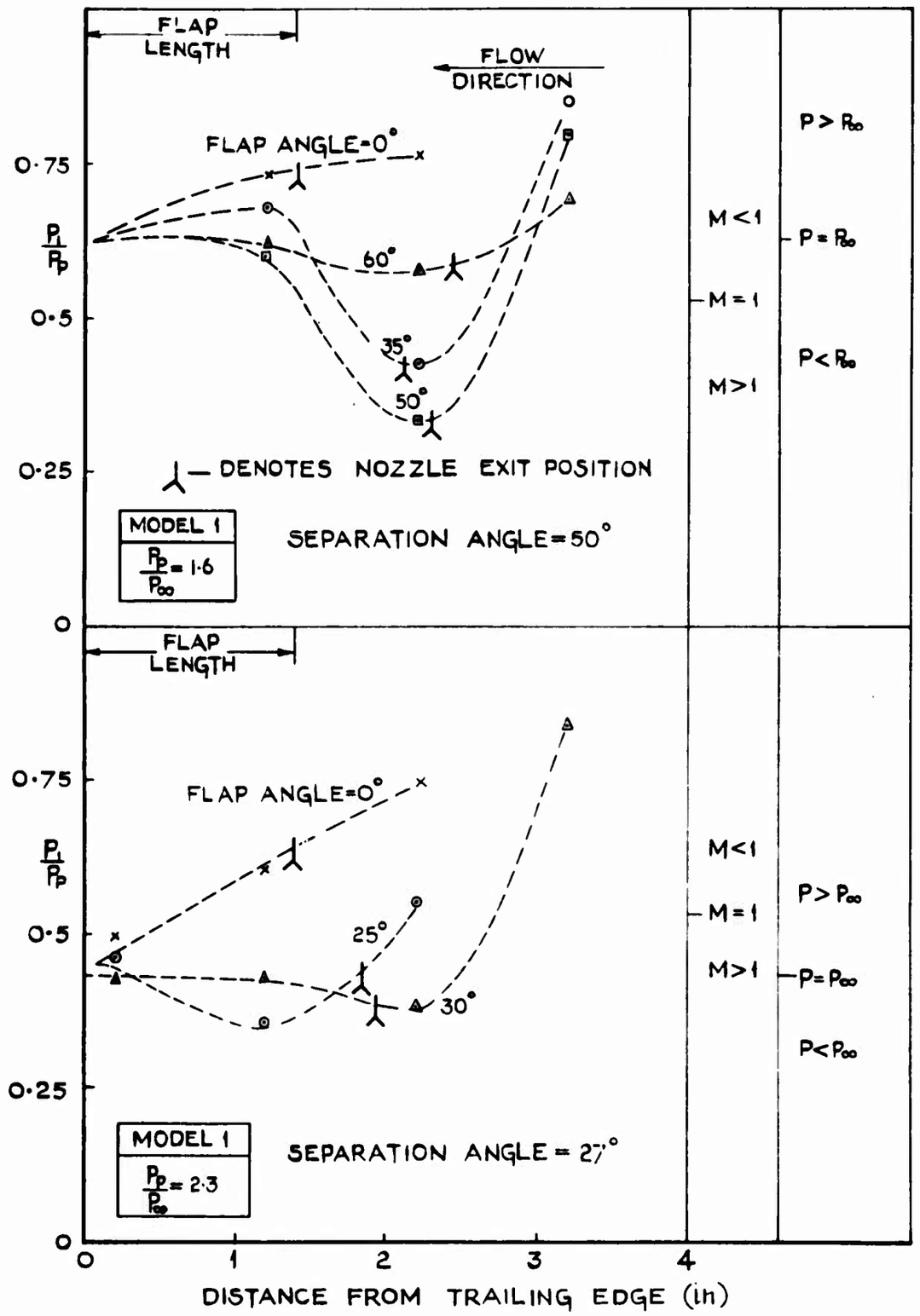

FIG. 6 STATIC PRESSURE DISTRIBUTION ON THE DEFLECTING SURFACE

Fig.7&8

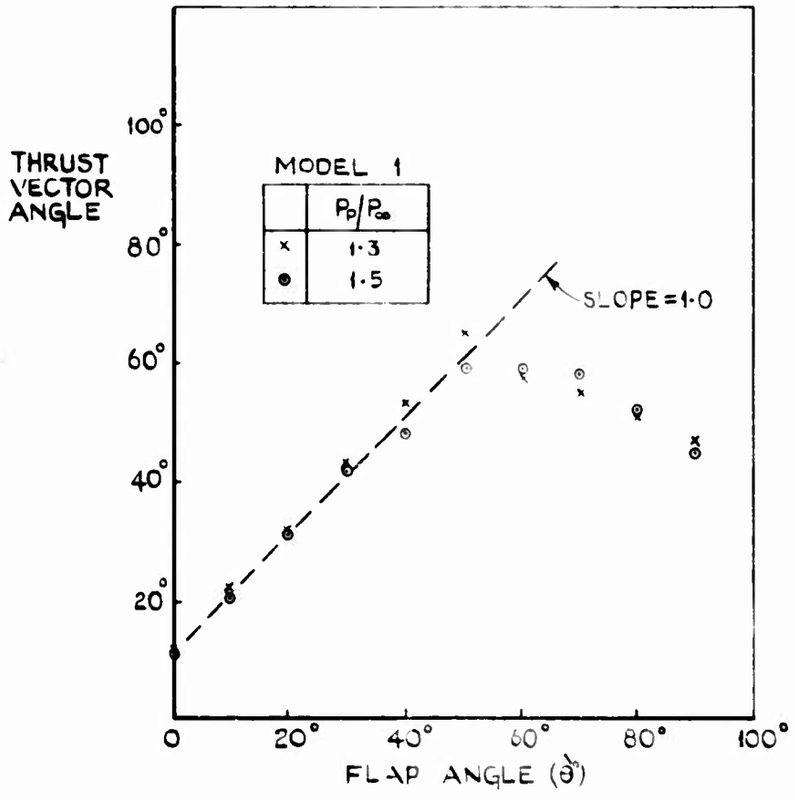

FIG. 7 THE THRUST VECTOR ANGLE – FLAP ANGLE RELATIONSHIP – R/h = 2

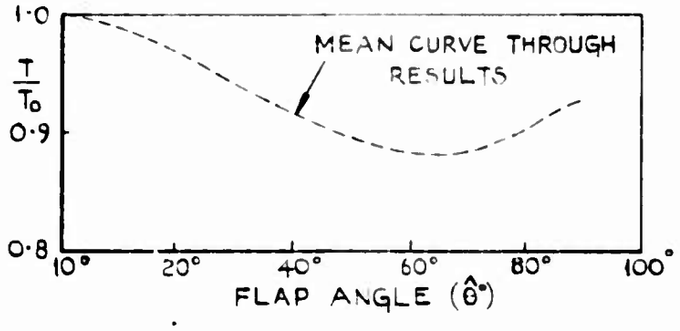

FIG.8 RATIO OF THRUST (T) TO THRUST AT ZERO FLAP ANGLE – R/h = 2

Fig.9

473565

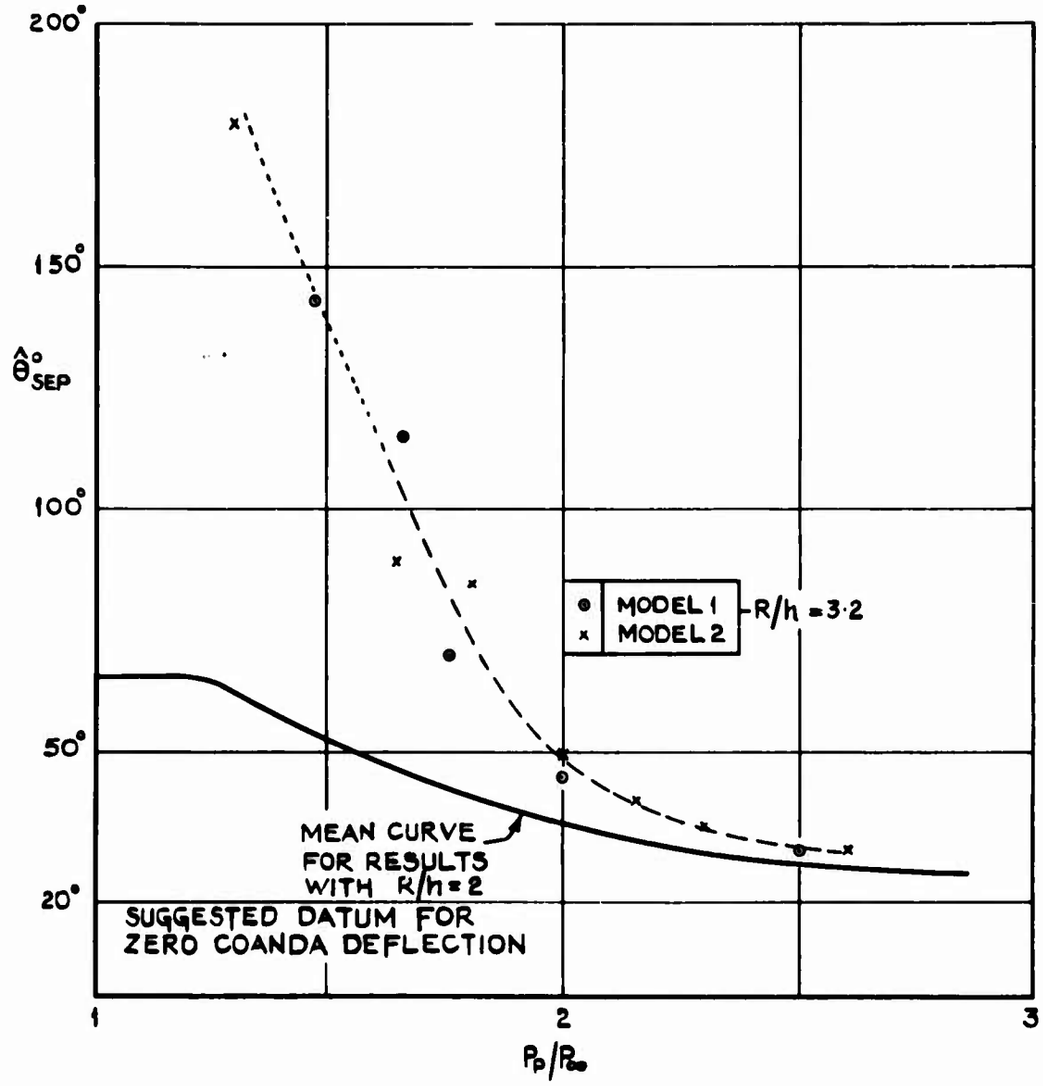

FIG.9 FLAP ANGLE AT SEPARATION – R/h = 3·2

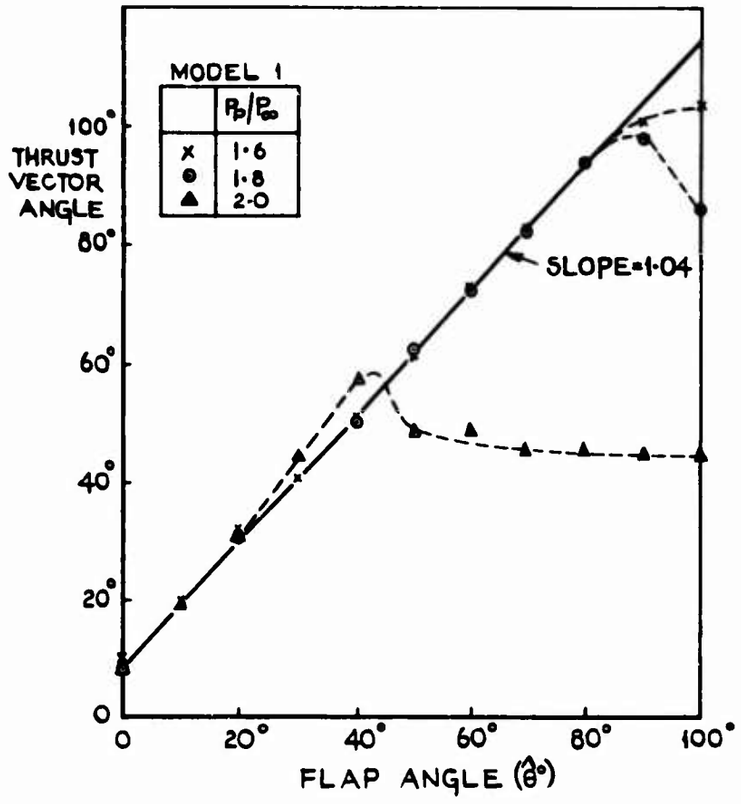

FIG. 10 THE THRUST VECTOR ANGLE — FLAP ANGLE RELATIONSHIP — R/h = 3·2

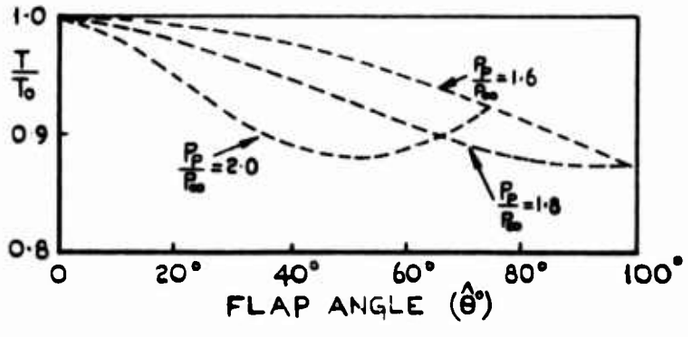

FIG. 11 RATIO OF THRUST (T) TO THRUST AT ZERO FLAP ANGLE — R/h = 3·2

Fig.12

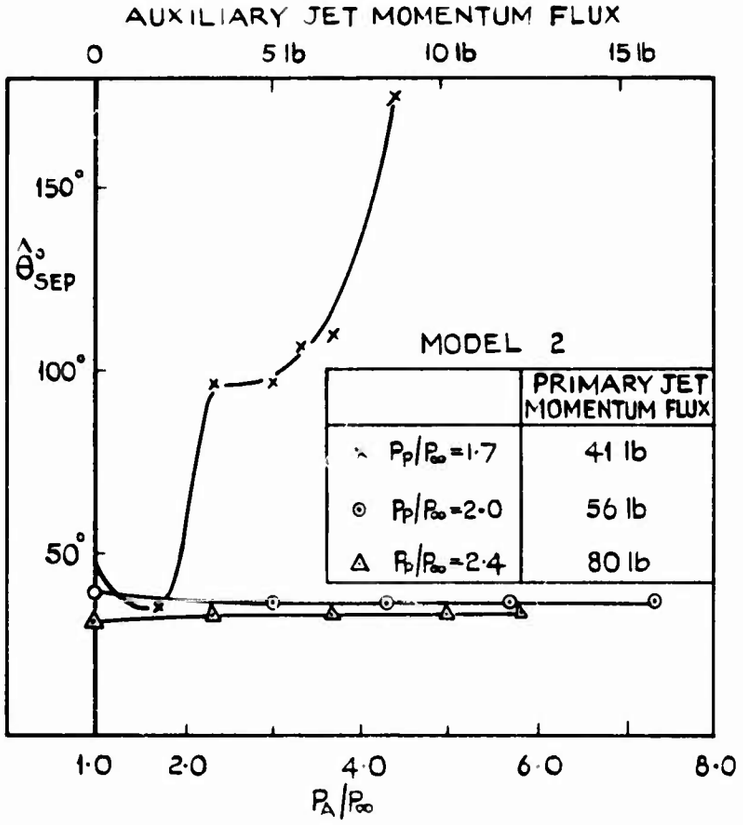

(a) MODEL 2

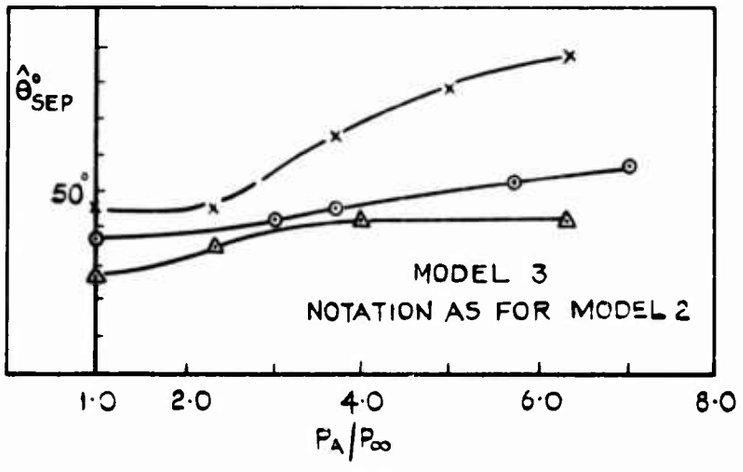

(b) MODEL 3

FIG. 12 THE EFFECT OF AN AUXILIARY JET ON THE FLAP ANGLE AT SEPARATION